Guest molecule entrapment by both capsule and hydrocarbon sidechains in self-assembled pyrogallol[4]arenes†‡

Oleg V. Kulikov,[a] Nigam P. Rath,[a] Dan Zhou,[b] I. Alexandru Carasel[c] and George W. Gokel[abc]

Received (in Montpellier, France) 23rd December 2008, Accepted 21st April 2009
First published as an Advance Article on the web 5th May 2009
DOI: 10.1039/b823160e

The self-assembly of pyrogallol[4]arenes resulted in the formation of hexameric capsules that trapped guest molecules present in solution, either within the capsule or within the pendant hydrocarbon chains. The results of analytical studies using FT-IR, ^{1}H NMR, ^{13}C NMR, TEM, TGA and HPLC are presented, along with the solid state structures of three hexameric capsules. Each of the capsules described has a large interior and includes various guest molecules.

Introduction

During the past half century, many novel theories have been advanced concerning the origins of life. An early and influential experiment was reported by Miller in 1953, in which he showed that amino acids resulted when the conditions of an early earth (Haldane's primordial soup) were emulated (the "Miller–Urey experiment").[1] These and subsequent results from this laboratory dominated thinking about the origins of life for some time. More recently however, alternate hypotheses and experimental evidence have emerged.[2] Prominent among these is Cairns-Smith's postulate that clay minerals produced self-replicating systems.[2a] Ferris and co-workers have provided experimental evidence relevant to this hypothesis.[3] De Duve has suggested that energetic thioester bonds were critical in initiating RNA-like polymer formation.[4] Orgel,[5] Eschenmoser[6] and their co-workers have also contributed to the RNA origin area. Wächtershäuser has been an advocate of the so-called "iron–sulfur world" in a metabolism-oriented description of the origins of life.[7] Luisi *et al.* have extensively studied liposomes, and suggested that the self-assembly and replication of liposomes is critical to the origins of life.[8a]

Although metabolism and reproduction are obviously both critical to the development of life, our interest has been in how the earliest organisms were enclosed and connected so that more elaborate systems could form. Our studies of synthetic ion channel systems arose from an interest in how encapsulated primordial organisms could communicate with the external environment.[8b,c] Of course, the function of channels is only required if there is encapsulation. In considering this conundrum, we were drawn to the recent studies of pyrogallolarenes, which self-assemble into capsules that appear to us to have pseudo-membrane hydrocarbon chains on the their surfaces. The capsules of interest form from pyrogallol and aldehydes in a reaction that is akin to the early phenol–formaldehyde condensations of Baekelund.[9] Such chemistry has also been used to form the cyclic condensates known as calixarenes.[10] The unusual feature of the pyrogallol tetramers is that they self-assemble into stable, hexameric, hydrogen-bonded capsules that enclose significant volumes.[11–14]

Most of the structural information concerning these large entities is derived from X-ray analyses. Solid state structures have been reported for the following *C*-alkylpyrogallolarenes: methyl,[13] propyl,[11] isobutyl,[13–15] butyl,[16,17] pentyl-heptyl[12,17] and octyl to undecyl.[16] Although the self-assembled capsules are highly organized, when they are decorated by alkyl chains of about ten or more members, their solid state structures are difficult to refine. This is because the hydrocarbon chains reduce the overall rigidity of the capsules and because the alkyl chains can exist in many different conformations. In addition to solid state structure determination, several recent papers have used diffusion NMR,[18] fluorescence[19] or gas phase mass spectrometry studies[20] to characterize pyrogallolarenes.

An interesting aspect of hydrogen-bonded capsule chemistry is their ability to incorporate guest molecules, such as fluorescent pyrenebutyric acid or 1-(9-anthryl)-3-(4-dimethyl-aniline)-propane (ADMA),[19c,d] within them. The goal of the work presented here was to form capsules that were surrounded by hydrophobic sidechains to see if these chains could also capture guest molecules. Such guest–sidechain interactions would resemble the capture of molecules by membranes. We report the solid state structures of three capsules that have pendant sidechains, and studies that demonstrate both encapsulation and surface capture. We also note that some structurally similar capsules have recently been reported.[16]

Results and discussion

The nomenclature system used in this paper is as follows. The pyrogallolarene is a tetramer formed from aldehyde and

[a] *Departments of Chemistry & Biochemistry and Biology, University of Missouri-St. Louis, St. Louis, MO 63121, USA*
[b] *Center for NanoScience, University of Missouri-St. Louis, St. Louis, MO 63121, USA*
[c] *Washington University, St. Louis, MO 63121, USA*

† Dedicated to Professor J. Rebek, Jr. and Professor J. de Mendoza on the occasion of their 65th birthdays.

‡ Crystal data for the structures in this paper have been deposited with the Cambridge Crystallographic Data Centre. CCDC 701456–701458. For crystallographic data in CIF or other electronic format see DOI: 10.1039/b823160e

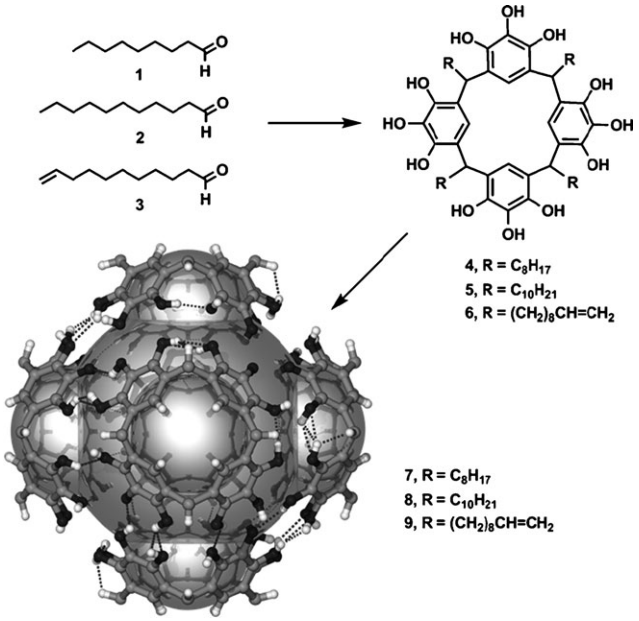

Scheme 1 The preparation of capsules **7–9**. Sidechains are not shown for clarity.

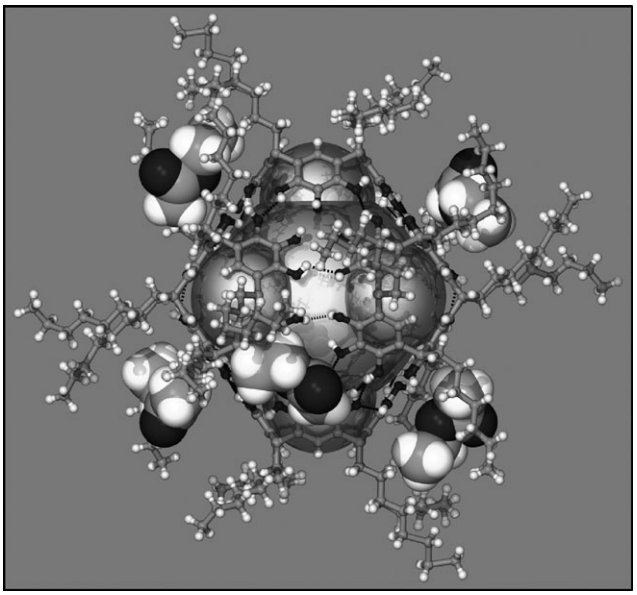

Fig. 1 The structure of nanocapsule **7** surrounded by six EtOAc molecules.

pyrogallol. When six of these tetramers organize into a discrete assembly, the resulting structure is referred to as a capsule. Capsules are usually characterized by X-ray analysis, as most analytical parameters are similar to those of other aggregates. When the tetramer crystallizes, it forms a solid that is often characterized by X-ray analysis as a bilayer. Alternately, the tetramer may crystallize into a dimeric capsule, also characterized by X-ray analysis. When we use the term "bilayer" below, we refer to the material that has crystallized but that is not known to be a capsule; typically, it appears to be a bilayer in the solid state. The use of the term bilayer to describe a substance in solution refers to the origin of the material and is not meant to indicate any level of organization in solution.

Treatment of pyrogallol with *n*-nonanal, *n*-undecanal and 10-undecenal, in the presence of HCl and EtOH, gave [4 + 4] condensation products *C*-octylpyrogallol[4]arene[16] **4** (35%), *C*-decylpyrogallol[4]arene[16] **5** (41%) and *C*-(9-decenyl)pyrogallol-[4]arene[21] **6** (40%), respectively. Crystallization of **4–6** from a 1 : 1 mixture (v/v) of CH_3CN : EtOAc gave the respective hexameric nanocapsules **7–9**, as shown in Scheme 1.

At least three attempts have been reported to study **4** by using X-ray diffraction analysis. Atwood and co-workers[17] reported a dimer obtained by the crystallization of **4** from CH_3CN containing 1 equivalent of H_2O. Nanocapsules were obtained by crystallization from EtOAc.[16] Mattay and co-workers[22] obtained a layered structure after crystallization from EtOH. Nanocapsule formation from *C*-decylpyrogallol-[4]arene has also been reported.[16] A search of the Cambridge Structural Database confirmed to us that the X-ray structure reported here is the first known for **6**.

Sidechain-trapped solvent

The central portion of any pyrogallarene capsule is similar. Variations in sidechain length have recently been shown by Cave *et al.*[16] to increase the intracapsular distance in an approximately linear fashion as the chain length increases from *n*-heptyl to *n*-undecyl. As the hydrocarbon chains increase in length, it becomes more likely that solvent will be trapped within the chains. The inclusion of solvent within a crystalline lattice is, of course, well known. In some cases, solvent shows a clear interaction with the compound of interest, and in others it appears to fill a void in the lattice. In further cases, disordered solvent is known to be present but its location is not unique. Solvent trapped within molecular capsules may be ordered or not, and examples of both have been reported. In examining the extracapsular chains, only ordered guest molecules can be confirmed.

The solid state structure of octyl sidechain capsule **7** is shown in Fig. 1.

Six ordered ethyl acetate (EtOAc) molecules are present in the exocapsular chains. In a structure reported previously,[16] **4** crystallized with one molecule of EtOAc atop the pyrogallol-arene and a second EtOAc was trapped within the alkyl chains. In the structure shown in Fig. 1, all six EtOAc molecules are positioned on the sides of the capsule. We infer an interaction between the alkyl chains and the ordered solvent molecules. As a practical matter, this cannot be distinguished from solvent so positioned within the lattice to fill a void.

The O···O distances for the hydroxyl hydrogen bonds of octyl sidechain nanocapsule **7** fall in the range 2.64–2.83 Å. These are typical hydrogen bond distances, implying that the capsule itself is organized as expected by the assembly of six pyrogallolarene molecules connected by 72 hydrogen bonds. We measured the intercapsular spacing as the shortest distance between the methine carbon atoms of neighboring capsules. The distance between adjacent capsules appears shorter than expected because the alkyl chains tend to spread to the sides rather than show either interdigitation or end-to-end contact.

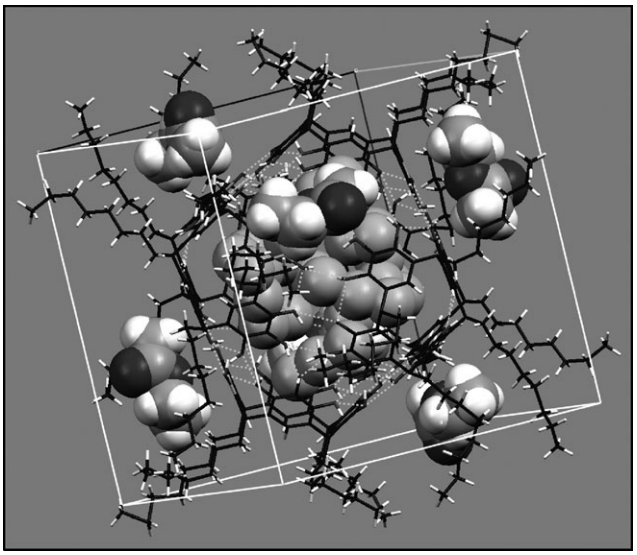

Fig. 2 A crystal packing diagram of nanocapsule **7**.

The shortest distance measured from a methine carbon in one capsule (**7**) to another was 4.7 Å. Cave *et al.*[16] computed the distance from the hypothetical center of one capsule to an adjacent one. This distance is ~21.7 Å for **7**.

The structure we obtained for **7** is similar to that reported by Cave *et al.*[16] In both cases, EtOAc molecules are held by the external chains. The present structure differs in that the solvent held in the extracapsular chains appears more ordered than previously reported. Perhaps as a result, the unit cell contains a single capsule and the unit cell volume for **7**·$(EtOAc)_6$ is 9940.0(7) Å^3 (see Fig. 2). This contrasts with the unit cell volume of 30 798(6) Å^3 for Cave *et al.*'s structure of **7**·$(EtOAc)_n$,[16] which contains at least two full capsules and elements of others. Fig. 2 is presented as a "stick" model, but the solvent molecules are shown in a space-filling representation. The six EtOAc molecules are obviously within the extracapsular chains. The spheres within the capsule show disordered H_2O molecules.

To our knowledge, capsule formation by crystallization from $CHCl_3$ has not previously been reported. When this was attempted and **4** (the tetramer) was deposited from $CHCl_3$ solution, a hexameric nanocapsule, presumably **7**, was obtained. Unfortunately, the diffraction data were poor. The data were, however, of sufficient quality to confirm the presence of capsule **7**, but only the first two carbon atoms of each alkyl chain could be refined (resolution ~2 Å). The resolution was sufficiently good, however, to show a regular hexameric capsule motif, and the presence of disordered $CHCl_3$ and H_2O, both inside the capsule and in the intercapsular space.

Single-crystal X-ray diffraction analyses of nanocapsules **8** (*n*-decyl sidechains) and **9** (*n*-9-decenyl sidechains) confirmed the formation of hexameric assemblies in both cases. Fig. 3 shows the solid state structures of decyl sidechain capsule **8** (left panel) and decenyl sidechain capsule **9** (right panel). The O···O distances for the hydroxyl hydrogen bonds of the pyrogallarene capsules fall in the expected range: 2.67–2.85 Å for **8** and 2.64–2.89 Å for **9**. The solid state structures are illustrated in Fig. 3.

Decylpyrogallolarene **8** has previously been reported by Cave *et al.*[16] The structural data suggested the presence of at least one EtOAc molecule within the capsule. In our hands, **8** crystallized with six molecules of EtOAc and six of CH_3CN (50% occupancy), all within the capsule. No solvent molecules were apparent within the *n*-decyl chains, although they may have been present and disordered. Although the solvent within the capsule was disordered, it is clear that six EtOAc molecules form an "outer shell", and that the CH_3CN molecules are organized within it (see Fig. 4). The carbonyl oxygen of each EtOAc was 3.06 Å from the nearest CH_3CN nitrogen atom. All six contact distances were identical.

Compound **9**, which has olefin-terminated 10-carbon chains, has not previously been reported. Its structure is shown in the right panel of Fig. 3. Within the capsule, however, six ordered EtOAc molecules are present (50% occupancy). The

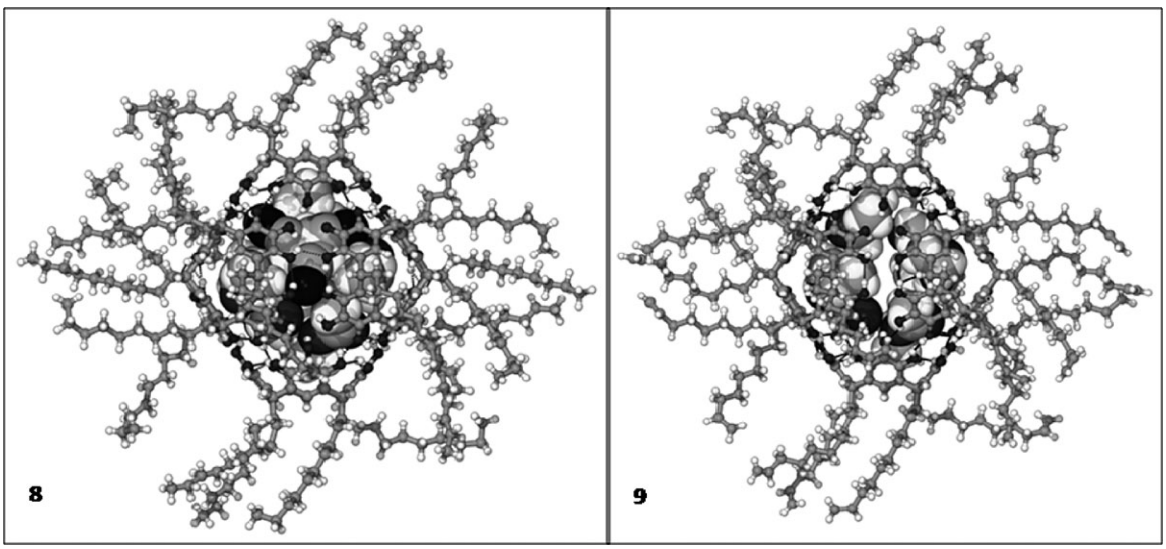

Fig. 3 The solid state structures of nanocapsules **8** (left) and **9** (right) with guests.

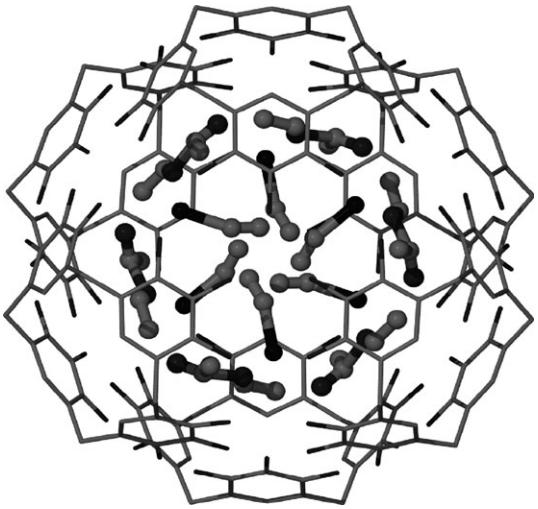

Fig. 4 The solid state structures of nanocapsule **8** showing the external ring of EtOAc molecules and CH_3CN guest matrix within it (viewed along the c axis). The sidechains are not shown for clarity.

carbonyl oxygen atom of each interacts with the hydrogen bond network of the capsule (the O···O distances are 2.99 Å). Also present within the capsule are disordered H_2O and EtOH molecules (all of them at 50% occupancy). Neither the exact number of each nor their orientation could be determined with precision. Disordered H_2O was identified outside the capsules, but no specific interactions with sidechains could be confirmed. The presence of EtOH molecules associated with the capsule is surprising as they must persist from the initial formation of the pyrogallolarene tetramer. The order in these crystals is greater than that observed for the decyl chains. This may be due to the greater rigidity of the terminal alkenes compared to ethyl groups.

Fig. 5 shows the partial crystal packing of nanocapsules **9**. The diameter of the circular array of seven molecules of **9** is ~113 Å or ~11 nm (the maximum distance between the alkyl chain's terminal carbons of capsules located on opposite sides of an array).

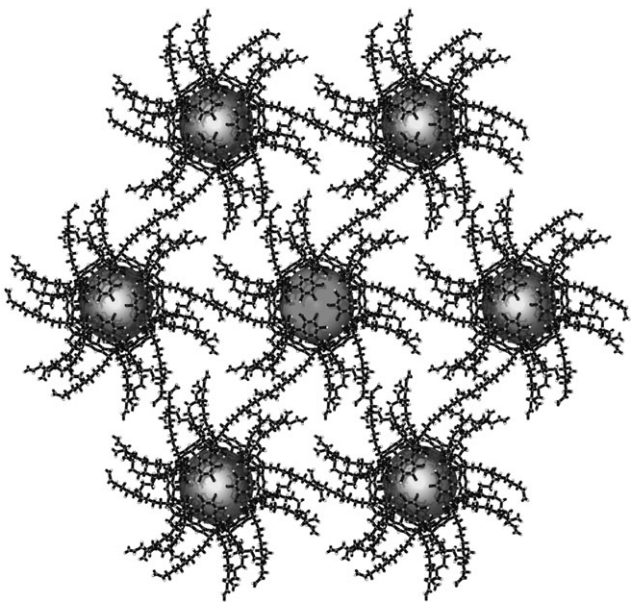

Fig. 5 A partial crystal packing diagram of nanocapsules **9** (viewed along the c axis).

The included volume reported by McGillivray and Atwood[23] for the first hexameric capsule based on *C*-methylresorcin[4]arene was 1375 $Å^3$. Atwood and co-workers have reported a range of included volume values for various pyrogallol[4]arene nanocapsules: ~1500 (propyl sidechain capsule),[11] 1510 (isobutyl sidechain capsule),[14] 1200 (hexyl sidechain capsule)[12] and 1300 $Å^3$ (pentyl and heptyl sidechain capsules).[12] Zhang *et al.* reported the volume of encapsulated space for methyl and isobutyl sidechain capsules to be 1490 and 1520 $Å^3$, respectively.[13] The interior volumes of hexameric nanocapsules **7**, **8** and **9**, reported here, were calculated by CAVITY[24] from solid state structural data to be 1239, 1209 and 1216 $Å^3$, respectively.

Thermogravimetric analysis

Thermogravimetric analysis (TGA) was conducted on *n*-decyl-sidechain capsule **8**. The solid state structure was best modelled with 6 EtOAc and 6 CH_3CN molecules within the capsule. When the temperature was raised to 110 °C, a weight loss of 8.2% was observed, which corresponds to ~610 Da. The molecular weights of CH_3CN and EtOAc are 41 and 88 Da, respectively. The weight loss could be accounted for by ~7 molecules of EtOAc or 15 molecules of CH_3CN; however, neither solvent is present in this quantity. Alternatively, 4 or 5 molecules of each solvent, respectively, have a weight of either 516 or 645 Da. It is unknown which solvent molecules account for the weight loss, but it must be a combination of both CH_3CN and EtOAc. The total mass of capsule **8** guests (6 EtOAc and 6 CH_3CN molecules) is ~774 Da. Upon heating to 265 °C, a further and final transition was observed, presumably the loss of the remaining solvent molecules and the decomposition of the assembly.

Microscopic examination of the nanocapsules

A transmission electron microscopic (TEM) examination of **9** was conducted as follows. Solutions of **9** in a 1 : 1 (v/v) mixture of EtOAc : CH_3CN were placed on a copper grid and allowed to evaporate for 20 min (see the Experimental section for additional details). The images shown in panels a–d of Fig. 6 demonstrate the range of aggregates that were observed. In panel a, small aggregates are apparent. The diameter of **9** is ~4 nm (40 Å). The wedge- or oval-shaped copper support is apparent in Fig. 6b, where the particle sizes are generally in the 200–300 nm range. Aggregates of ~30 nm diameter are apparent in the lower-left wedge in this panel. Fig. 6(c) shows particles in the 200–300 nm range in the upper-right wedge and mostly smaller particles (as small as ~25 nm) in the lower-left wedge. An extremely large aggregate (~1750 nm) was detected in the micrograph shown in panel d. A similar broad particle size range was observed for **7** and **8**, which have *n*-octyl and *n*-decyl sidechains, respectively (data not shown).

Atwood and co-workers[25] have reported TEM studies on pyrogallolarene capsules that have isobutyl sidechains. They observed a range of particle sizes, 92 ± 42 nm, although their aggregates were deposited from acetone. This range is

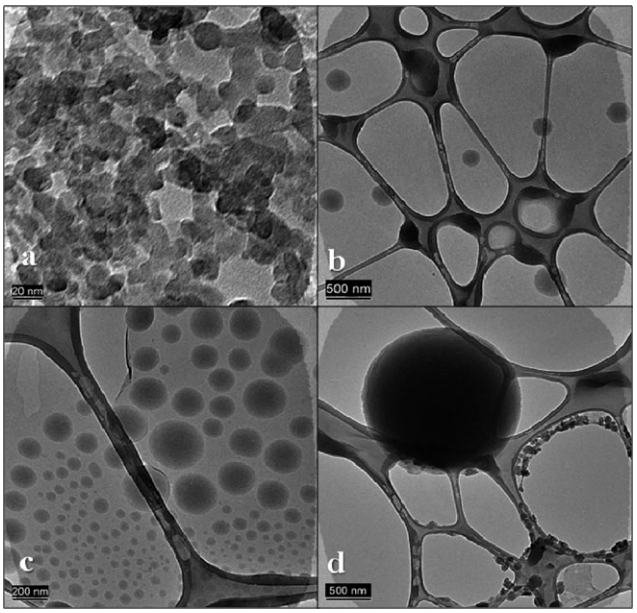

Fig. 6 TEM images of aggregates formed from capsule **9** dissolved in an EtOAc/CH_3CN solution and evaporated onto a copper grid (scale bars: 6a 20 nm, 6b 500 nm, 6c 200 nm and 6d 500 nm).

remarkably smaller than the one we observed for **9**. It seems possible that differences in concentration, solution aging or even evaporation times might account for the variation in aggregate sizes. In any event, it is clear that a far greater range of aggregate sizes is observed for **7**, **8** and **9** than for the isobutyl sidechain capsules. Although the solvents from which these aggregates were deposited differ, the dielectric constant of acetone is ~21 and the average dielectric constant of a 1 : 1 mixture of EtOAc (ε = 6) and CH_3CN (ε = 36) is also ~21. We speculate that the self-assembly of isobutyl sidechain capsules is dominated by large capsules, but that when long sidechains are present, they interact and interdigitate, as in bilayer membranes.

The initial goal of the TEM study was to image individual capsules. We note that an individual capsule has a spherical diameter of about 40 Å (4 nm, 0.04 μm). Although part of the image shown in Fig. 6a may be interpreted as an individual capsule, it is not clear enough to be convincing. The smallest particles observed upon dilution and sonication were found to be ~10 nm in size, which could roughly be attributed to the structure displayed in Fig. 5. Moreover, too few such small particles were detected to be sure that individual monomers were common. Using a diameter of 4 nm (40 Å) for an idealized sphere, we estimated that particles as small as 20 nm contained ~125 monomers. The vast number of monomers that must be present in particles having diameters of 200 to nearly 2000 nm is obvious. The extensive self-assembly of many monomers of **7–9** is a reasonable proposition if their sidechains interact in all three dimensions.

Aggregation and capsule formation dynamics

Pyrogallolarenes are inherently dynamic. The reaction of pyrogallol with an aldehyde gives a covalent macrocycle consisting of four arenes linked by four methylene groups.

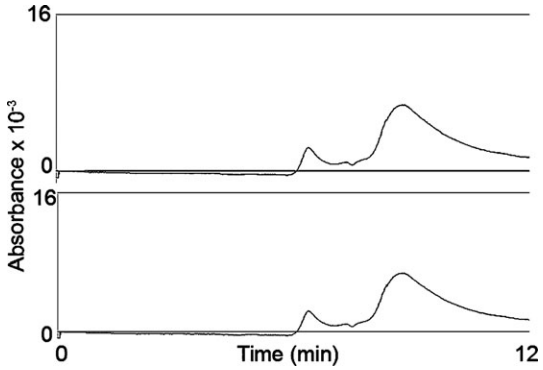

Fig. 7 HPLC traces in EtOAc for equal weights of C_{10} monomer **5** (added as a bilayer) (top panel) and C_{10} hydrogen-bonded capsule **8** (lower panel).

This tetramer is considered to be the pyrogallarene monomer. It may or may not be monomeric in solution, but it typically crystallizes either as a bilayer or it forms a solid capsule. Examples of the latter are shown above in Fig. 1–5. It is known empirically that certain solvents favor capsule formation. We wished to see if clear evidence could be obtained for the presumed solution equilibria. We therefore dissolved equal weights of C_{10}-bilayer and C_{10}-capsule (compound **8**) in EtOAc and analyzed them by HPLC. The experiments were conducted on an Xper-Chrom Model 1400 HPLC using a Shodex 5SIL 10E normal phase column (UV-vis detector, λ = 275 nm). The HPLC traces are shown in Fig. 7.

Each experiment was repeated at least three times with no significant variation. The near identical nature of the traces suggests that a complex equilibrium is established almost instantaneously. There appear to be two major peaks and two shoulders, rather than the expected six peaks. This might result from monomer (**5**), dimer ($\mathbf{5}_2$), tetramer ($\mathbf{5}_2$ + $\mathbf{5}_2$) and hexamer ($\mathbf{5}_6$ = **8**). The latter is speculative, but all or any of the self-assembled fragments, $\mathbf{5}_n$, are expected in the EtOAc solution. What can be inferred with certainty is that the pyrogallolarenes are in dynamic equilibrium and that the crystallization conditions are clearly critical to the formation of uniform entities, such as capsules, from the various solutions. We note that the signals recorded by the UV detector (λ = 275 nm) seemed weak. We attempted to determine the extinction coefficients (ε) for tetramer **5** in hexane, CH_2Cl_2, EtOAc, EtOH, MeOH and DMSO. The values we observed were solvent-dependent and, as the HPLC traces suggest, varied over time (data not shown). In all cases, ε was greater than the value reported for phenol in H_2O (1450 at 270 nm).[26] Our values were typically 3000, and differed from the data reported by Ursaleş *et al.*[27] They reported UV spectra in MeOH for ethyl, propyl and hexyl sidechain tetramers; the extinction coefficients at λ_{max} were: ethyl, 6300 at 284 nm; propyl, 7700 at 284 nm; and hexyl, 9600 at 278 nm. At present, we have no explanation for this difference.

Conclusions

Our initial goal in this study was to understand the effect of extended alkyl chains on the properties and organization of hydrogen-bonded pyrogallolarene capsules. Solid state

structural analyses of known **7** and **8**, and for previously unreported **9**, show that extended chains offer a "secondary" binding site for molecular guests. Thus far, only solvents have been incorporated, but their effect within the chains has been to produce more highly-organized structures, at least in the solid state. The second finding is that as the sidechains lengthen, the intermolecular interactions become more extensive. TEM shows that much larger aggregates form from longer-chained capsules than do so from, for example, the isobutyl sidechain capsules that were previously reported. The ability of the sidechains to form organized assemblies with guest molecules, and to interact strongly with each other, adds another dimension to the chemistry of these remarkable compounds. Finally, we have shown that a dynamic equilibrium exists between the formation of capsules from monomers and the de-aggregation of the capsules. The specific form observed in the solid state is likely to reflect both intermolecular forces associated with self-assembly and crystal packing forces.

Experimental section

All reagents, unless otherwise stated, were the highest grade commercially available and were used without further purification. *C*-Octylpyrogallol[4]arene **4**, *C*-decylpyrogallol-[4]arene **5** and *C*-(9-decenyl)pyrogallol[4]arene **6** were prepared as described in the literature.[16,21] ^{1}H and ^{13}C NMR spectra were recorded at 300 MHz or 75 MHz in $CDCl_3$, and are reported in ppm. TGA experiments were performed on a Q500 instrument. Micrographs were recorded on a JEOL EM-2000FX electron microscope operating at 200 kV. Nanocapsules **7–9** were supported on a "holey" carbon film. The carbon coated copper grid was dipped once into a stock solution containing the nanocapsule in 1 : 1 (v/v) EtOAc : CH_3CN and allowed to dry in air (ambient temperature) for 20 min.

Single-crystal X-ray analyses

Crystals with approximate dimensions 0.42 × 0.33 × 0.27 mm^3 (for nanospheroid **7**), 0.32 × 0.21 × 0.11 mm^3 (for nanospheroid **8**) and 0.28 × 0.22 × 0.12 mm^3 (for nanospheroid **9**) were mounted on glass fibers in random orientations. Preliminary examinations and data collections were performed using a Bruker Kappa Apex II CCD detector single-crystal X-ray diffractometer equipped with an Oxford Cryostream LT device. All data were collected using graphite-monochromated Mo-K_α radiation (wavelength λ = 0.71073 Å) from a fine focus sealed tube X-ray source. Preliminary unit cell constants were determined with a set of 36 narrow frame scans. Typical data sets consisted of combinations of ω and f scan frames, with a typical scan width of 0.5° and a counting time of 30–60 sec frame^{-1} at a crystal to detector distance of 4.0 cm. The collected frames were integrated using an orientation matrix determined from the narrow frame scans. Apex II and SAINT software packages[28] were used for data collection and integration. Analysis of the integrated data did not show any decay. Collected data were corrected for systematic errors using SADABS, based on the Laue symmetry using equivalent reflections. Structure solution and refinement were carried out using the SHELXTL-PLUS software package.[29] The structures were solved by direct methods and refined successfully in the space group *R*-3 (for all capsules **7–9**). Full matrix least-squares refinement was carried out by minimizing $\Sigma w(F_o^2 - F_c^2)^2$. Most of the non-hydrogen atoms of the crown were refined anisotropically to convergence. Rigid body refinement (AFIX 6) was used for some of the solvent molecules and aliphatic chains. All hydrogen atoms were treated using the appropriate riding model (AFIX m3). While the gross non-hydrogen connectivities have been established, no great reliance should be placed on the reported hydrogen atom coordinates on the markedly prolate carbon atoms in the octyl **7**, decyl **8** and decenyl **9** chains of these compounds. Also, in capsule **9**, the terminal unit occupancy carbon site C68 (which could only be refined isotropically) is not reliable, as it is only 2.23 and 2.34 Å from the adjacent half-occupancy water O5S sites.

C-Octylpyrogallol[4]arene hexameric nanocapsule 7

C-Octylpyrogallol[4]arene (**4**, 150 mg) was dissolved in EtOAc (5 mL) and CH_3CN (5 mL) was added. Slow evaporation at ambient temperature over several days afforded yellowish crystals. ^{1}H NMR: 0.91 (t, J = 6.6 Hz, 12H, CH_3), 1.24–1.31 (m, 48H, $(CH_2)_6$), 2.02 (s, CH_3CO, EtOAc), 2.05 (s, CH_3, CH_3CN), 2.23 (m, 8H, CHCH_2), 4.12 (q, J = 7.1 Hz, CH_2CH$_3$, EtOAc), 4.38 (t, J = 7.5 Hz, 4H, Ar$_2$C*H*CH$_2$, methine), 6.85 (s, 4H, Ar*H*), 6.89 (s, 4H, ArO*H*), 7.48 (s, 4H, ArO*H*) and 8.79 (s, 4H, ArO*H*). ^{13}C NMR: 2.06, 14.33, 14.39, 21.23, 22.92, 28.45, 29.56, 29.91, 30.09, 32.11, 33.35, 34.31, 60.58, 114.02, 124.29, 125.61, 131.59, 137.57, 138.71 and 171.33. FT-IR (solid): ν = 975, 1090, 1118, 1238, 1280, 1337, 1474, 1507, 1633, 1732 (C═O, EtOAc), 2855, 2924, 3249 and 3458 cm^{-1}.

Nanocapsules grown from EtOAc : CH_3CN (1 : 1, v/v). $C_{64}H_{102}O_{17}$, M = 1143.46, rhombohedral, space group *R*-3, a = 21.5048(9), b = 21.5048(9), c = 21.5048(9) Å, α = 91.042(11)°, U = 9940.0(7) Å^3, μ = 0.082 mm^{-1}, T = 100(2) K, Z = 6, GOF = 1.469, final *R*-indices (R_1 = 0.1669, wR_2 = 0.4226), 98 900 reflections collected, 11 656 unique (R_{int} = 0.23), su 0.11, the equivalent hexagonal cell is: 30.688(11), 30.688(11), 36.564(32); 90.00, 90.00, 120.00. U = 29820.29 Å^3. CCDC 701456.‡

Nanocapsules grown from $CHCl_3$. $C_{61}H_{89}Cl_3O_{12}$, M = 1120.67, a = 30.1971(15), b = 30.1971(15), c = 39.411(4) Å, α = 90.00, β = 90.00, γ = 120.00°, U = 31123(4) Å^3, μ = 0.184 mm^{-1}, T = 100(2) K, Z = 18. These data were not submitted to the CSD owing to disorder that prevented structure refinement.

C-Decylpyrogallol[4]arene hexameric nanocapsule 8

C-Decylpyrogallol[4]arene (**5**, 200 mg) was dissolved in EtOAc (5 mL) and CH_3CN (5 mL) was added. Slow evaporation at ambient temperature over several days afforded yellowish crystals. ^{1}H NMR: 0.89 (t, J = 6.2 Hz, 12H, CH_3), 1.24–1.29 (m, 64H, $(CH_2)_8$), 2.02 (s, CH_3CO, EtOAc), 2.05 (s, CH_3, CH_3CN), 2.23 (m, 8H, CHCH_2), 4.12 (q, CH_2CH$_3$, EtOAc), 4.38 (t, J = 7.1 Hz, 4H, Ar$_2$C*H*CH$_2$, methine), 6.84

(s, 4H, ArH), 6.89 (s, 4H, ArOH), 7.48 (s, 4H, ArOH) and 8.79 (s, 4H, ArOH). ^{13}C NMR: 2.08, 14.32, 14.41, 21.25, 22.92, 28.49, 29.64, 29.91, 29.96, 30.02, 30.14, 32.19, 33.39, 33.84, 34.34, 60.59, 114.01, 124.29, 125.61, 131.59, 137.57, 138.71 and 171.35. FT-IR (solid): ν = 970, 1096, 1277, 1337, 1480, 1507, 1627, 1726 (C=O, EtOAc), 2844, 2921, 3271 and 3447 cm^{-1}.

$C_{146}H_{227}NO_{28}$, M = 2444.29, rhombohedral, space group R-3, a = 37.210(2), b = 37.210(2), c = 25.915(4) Å, U = 31075(5) Å^3, μ = 0.080 mm^{-1}, T = 100(2) K, Z = 9, GOF = 1.601, final R-indices (R_1 = 0.1898, wR_2 = 0.4486), 186 526 reflections collected, 10865 unique (R_{int} = 0.24). CCDC 701457.‡

C-(9-Decenyl)pyrogallol[4]arene hexameric nanocapsule 9

C-(9-Decenyl)-pyrogallol[4]arene (**9**, 200 mg) was dissolved in EtOAc (5 mL) and CH_3CN (5 mL) was added. Slow evaporation at ambient temperature over several days afforded crystals. ^{1}H NMR: 1.25–1.38 (m, 48H, $(CH_2)_6$), 2.01–2.07 (m, CH_2–CH=CH_2, 8H; CH_3CO, EtOAc; CH_3, CH_3CN), 2.24 (m, 8H, $CHCH_2$), 4.12 (q, CH_2CH_3, EtOAc), 4.38 (t, 4H, Ar_2CHCH_2, methine), 4.93–5.09 (m, CH_2–CH=CH_2, 8H), 5.76–5.89 (m, CH_2–CH=CH_2, 8H), 6.85 (s, 4H, ArH), 6.89 (s, 4H, ArOH), 7.48 (s, 4H, ArOH) and 8.79 (s, 4H, ArOH). ^{13}C NMR: 14.40, 21.24, 28.47, 29.20, 29.39, 29.75, 29.95, 30.09, 33.38, 34.04, 34.31, 60.60, 113.99, 114.36, 124.29, 125.60, 131.60, 137.58, 138.72, 139.37 and 171.36. FT-IR (solid): ν = 904, 975, 1074, 1238, 1277, 1337, 1474, 1512, 1638, 1721 (C=O, EtOAc), 2844, 2921, 3260 and 3452 cm^{-1}.

$C_{71}H_{110}O_{15}$, M = 1203.59, rhombohedral, space group R-3, a = 37.052(2), b = 37.052(2), c = 25.8772(19) Å, U = 30767(4) Å^3, μ = 0.080 mm^{-1}, T = 100(2) K, Z = 18, GOF = 1.335, final R-indices (R_1 = 0.1301, wR_2 = 0.3501), 138 722 reflections collected, 12047 unique (R_{int} = 0.17). CCDC 701458.‡

High performance liquid chromatography

HPLC experiments were conducted on a Xper-Chrom Model 1400 HPLC equipped with a UV-vis detector (λ = 275nm) using a Shodex 5SIL 10E normal phase column. Experiments were performed at least in duplicate, and traces were recorded using Peak Simple v. 2.08 software. Samples were dissolved in EtOAc, and the mobile phase was also EtOAc.

Determination of extinction coefficients

Extinction coefficients were determined by recording the UV-vis spectrum of a sample of known weight dissolved in hexanes, CH_2Cl_2, EtOH, MeOH or DMSO. All solvents were of the highest grade obtainable.

Acknowledgements

We gratefully acknowledge grants from the NIH (GM-36262) and NSF (04-20497) that supported this work.

References

1 S. L. Miller, *Science*, 1953, **117**, 528.
2 (*a*) A. G. Cairns-Smith, *Seven Clues to the Origin of Life A: Scientific Detective Story*, Canto-Cambridge University Press, Cambridge, UK, 1985; (*b*) F. Dyson, *Origins of Life*, Cambridge University Press, Cambridge, UK, 2nd edn, 1999.
3 (*a*) N. G. Holm, A. G. Cairns-Smith, R. M. Daniel, J. P. Ferris, R. J. Hennet, E. L. Shock, B. R. Simoneit and H. Yanagawa, *Origin Life Evol. Biosph.*, 1992, **22**, 181; (*b*) J. P. Ferris and G. Ertem, *J. Am. Chem. Soc.*, 1993, **115**, 12270.
4 C. de Duve, *Gene*, 1993, **135**, 29.
5 L. E. Orgel, *Nature*, 2006, **439**, 915.
6 G. K. Mittapalli, Y. M. Osornio, M. A. Guerrero, K. R. Reddy, R. Krishnamurthy and A. Eschenmoser, *Angew. Chem., Int. Ed.*, 2007, **46**, 2478.
7 (*a*) G. Wächtershäuser, *Proc. Natl. Acad. Sci. U. S. A.*, 1994, **91**, 4283; (*b*) G. Wächtershäuser, in *Thermophiles: The Keys to Molecular Evolution and the Origin of Life*, ed. J. Wiegel and M. W. W. Adams, Taylor & Francis Ltd., London, UK, 1998, pp. 47.
8 (*a*) K. Morigaki, S. Dallavalle, P. Walde, S. Colonna and P. L. Luisi, *J. Am. Chem. Soc.*, 1997, **119**, 292; (*b*) G. W. Gokel, *Chem. Commun.*, 2000, 1; (*c*) G. W. Gokel, P. H. Schlesinger, N. K. Djedovic, R. Ferdani, E. C. Harder, J. Hu, W. M. Leevy, J. Pajewska, R. Pajewski and M. E. Weber, *Bioorg. Med. Chem.*, 2004, **12**, 1291.
9 L. H. Baekelund, *US Pat.*, 0,942,809, issued December 7, 1909.
10 C. D. Gutsche, *Calixarenes Revisited*, Royal Society of Chemistry, Cambridge, UK, 1998, vol. 6.
11 J. L. Atwood, L. J. Barbour and A. Jerga, *J. Supramol. Chem.*, 2001, **1**, 131.
12 G. W. Cave, J. Antesberger, L. J. Barbour, R. M. McKinlay and J. L. Atwood, *Angew. Chem., Int. Ed.*, 2004, **43**, 5263.
13 Q.-F. Zhang, R. D. Adams and D. Fenske, *J. Inclusion Phenom. Macrocyclic Chem.*, 2005, **53**, 275.
14 J. L. Atwood, L. J. Barbour and A. Jerga, *Chem. Commun.*, 2001, 2376.
15 T. Gerkensmeier, W. Iwanek, C. Agena, R. Fröhlich, S. Kotila, C. Näther and J. Mattay, *Eur. J. Org. Chem.*, 1999, 2257.
16 G. W. V. Cave, S. J. Dalgarno, J. Antesberger, M. C. Ferrarelli, R. M. McKinlay and J. L. Atwood, *Supramol. Chem.*, 2008, **20**, 157.
17 S. J. Dalgarno, J. Antesberger, R. M. McKinlay and J. L. Atwood, *Chem.–Eur. J.*, 2007, **13**, 8248.
18 (*a*) T. Evan-Salem and Y. Cohen, *Chem.–Eur. J.*, 2007, **13**, 7659; (*b*) L. Avram and Y. Cohen, *Org. Lett.*, 2006, **8**, 219; (*c*) L. Avram and Y. Cohen, *J. Am. Chem. Soc.*, 2005, **127**, 5714; (*d*) L. Avram and Y. Cohen, *J. Am. Chem. Soc.*, 2003, **125**, 16180; (*e*) I. Philip and A. E. Kaifer, *J.Org. Chem.*, 2005, **7**, 1558; (*f*) L. Avram and Y. Cohen, *J. Am. Chem. Soc.*, 2004, **126**, 11556; (*g*) L. C. Palmer and J. Rebek, Jr., *Org. Lett.*, 2005, **7**, 787; (*h*) L. Avram and Y. Cohen, *Org. Lett.*, 2003, **5**, 3329; (*i*) Y. Cohen, T. Evan-Salem and L. Avram, *Supramol. Chem.*, 2008, **20**, 71.
19 (*a*) E. S. Barrett, T. J. Dale and J. Rebek, Jr., *Chem. Commun.*, 2007, 4224; (*b*) E. S. Barrett, T. J. Dale and J. Rebek, Jr., *J. Am. Chem. Soc.*, 2008, **130**, 2344; (*c*) D. B. Bassil, S. J. Dalgarno, G. W. V. Cave, J. L. Atwood and S. A. Tucker, *J. Phys. Chem. B*, 2007, **111**, 9088; (*d*) S. J. Dalgarno, S. A. Tucker, D. B. Bassil and J. L. Atwood, *Science*, 2005, **309**, 2037.
20 N. K. Beyeh, M. Kogej, A. Ahman, K. Rissanen and C. A. Schalley, *Angew. Chem., Int. Ed.*, 2006, **45**, 5214.
21 E. U. Thoden van Velzen, J. F. J. Engbersen and D. N. Reinhoudt, *Synthesis*, 1995, **8**, 989.
22 T. Gerkensmeier, C. Agena, W. Iwanek, R. Fröhlich, S. Kotila, C. Näther and J. Mattay, *Z. Naturforsch.*, 2001, **56b**, 1063.
23 L. R. McGillivray and J. L. Atwood, *Nature*, 1997, **389**, 469.
24 L. J. Barbour, *CAVITY*, unpublished computer program, University of Stellenbosch, South Africa.
25 M. W. Heaven, G. W. V. Cave, R. M. McKinlay, J. Antesberger, S. J. Dalgarno, P. K. Thallapally and J. L. Atwood, *Angew. Chem., Int. Ed.*, 2006, **45**, 6221.
26 P. Crews, J. Rodriguez and M. Jaspars, *Organic Structure Analysis*, Oxford University Press, New York, 1998, pp. 362.
27 T.-N. Ursaleş, E.-J. Popovici, G.-N. Nemes and N. Popovici, *Acta Univ. Cibiniensis, Ser. F: Chim.*, 2002, **5**, 63.
28 Bruker Analytical X-Ray, Madison, WI, USA, 2006.
29 Bruker-SHELXTL: G. M. Sheldrick, *Acta Crystallogr., Sect. A: Fundam. Crystallogr.*, 2008, **64**, 112.